Calorimetric Unfolding of Intramolecular Triplexes: Length Dependence and Incorporation of Single AT → TA Substitutions in the Duplex Domain

Ronald Shikiya[†] and Luis A. Marky*[,†,‡]

Departments of Pharmaceutical Sciences and Biochemistry and Molecular Biology and Eppley Institute for Cancer Research, University of Nebraska Medical Center, 986025 Nebraska Medical Center, Omaha, Nebraska 68198

Received: May 4, 2005; In Final Form: July 27, 2005

DNA triplexes have been the subject of great interest due to their ability to interfere with gene expression. The inhibition of gene expression involves the design of stable triplexes under physiological conditions; therefore, it is important to have a clear understanding of the energetic contributions controlling their stability. We have used a combination of UV spectroscopy and differential scanning calorimetric (DSC) techniques to investigate the unfolding of intramolecular triplexes, $d(A_nC_5T_nC_5T_n)$, where n is 5−7, 9, and 11, and related triplexes with a single AT → TA substitution in their duplex stem. Specifically, we obtain standard thermodynamic profiles for the unfolding of each triplex in buffer solutions containing 0.1 M or 1 M NaCl. The triplexes unfold in monophasic or biphasic transitions (triplex → duplex → coil) depending on the concentration of salt used and position of the substitution, and their transition temperatures are independent of strand concentration. The DSC curves of the unsubstituted triplexes yielded an unfolding heat of 13.9 kcal/mol for a TAT/TAT base-triplet stack and a heat capacity of 505 cal/°C·mol. The incorporation of a single substitution destabilizes triplex formation (association of the third strand) to a larger extent in 0.1 M NaCl, and the magnitude of the effects also depends on the position of the substitution. The combined results show that a single AT → TA substitution in a homopurine/homopyrimidine duplex does not allow triplex formation of the neighboring five TAT base triplets, indicating that the in vivo formation of triplexes, such as H-DNA, is exclusive to homopurine/homopyrimidine sequences.

Introduction

The conclusion of the human genome project keeps changing the course and focus of research in pharmaceutical science.[1] Analysis of the human genome is increasing the development of new therapeutic drugs that could potentially target genes of interest, and their success relies on the mechanisms of discriminating sequences differing by a few nucleotides.[1] Nucleic acid molecules, as therapeutic drugs, possess a very high selectivity and are able to distinguish gene targets that differ on a single base.[2] Therefore, oligonucleotides (ODNs) could be employed to selectively regulate gene expression.[3−5] There are two main approaches for the use of ODNs as gene expression modulators: antisense and antigene strategies.[3] In the antisense approach, ODNs bind to a messenger RNA, forming DNA/RNA hybrid duplexes. The formation of this hybrid inhibits the translation of a given gene by sterically blocking the correct assembly of the translation machinery or by inducing an RNAse H mediated cleavage of their mRNA target.[3] In the antigene approach, an ODN binds into the major groove of a DNA duplex, forming a local triple helix.[6,7] The third strand competes with the proteins that activate the transcription machinery by forming a triplex complex, thus inhibiting the expression of a specific gene.[4,8]

Since the antigene strategy targets the gene directly, one advantage of this approach over its antisense counterpart is the fewer number of copies of the gene of interest. In addition, blocking the transcription of a gene itself prevents the turnover of the mRNA pool, allowing a more efficient and lasting inhibition of gene expression.[5] However, disadvantages for this strategy are that ODNs need to cross the nuclear membrane and access the targeted gene within the densely packed chromatin structure.[9,10]

Furthermore, the interaction of a third strand with a DNA duplex is sequence specific, allowing the recognition of different DNA targets by Hoogsteen base pairing.[6,7] These triplexes are stabilized by base-triplet stacking interactions and hydrogen bonding between the bases of the third strand and the purine bases of the duplex.[11] Triplexes are classified on the basis of the composition and orientation of their third strand, which is placed asymmetrically in the major groove of the target duplex and closer to the purine strand. For example, the third strand of parallel triplexes ("pyrimidine" motif) is usually pyrimidine rich and binds parallel to the purine strand of the duplex. On the other hand, the third strand of antiparallel triplexes ("purine" motif) is purine rich and binds the duplex purine strand in the antiparallel orientation.[7,12,13] The resulting base triplets have an isomorphous topology; that is, they are superimposable, allowing a regular conformation of the sugar−phosphate backbone.[7] In addition, a duplex molecule has to have a homopurine/homopyrimidine sequence in order for a third strand to form a stable triplex complex. Moreover, the use of triplex molecules as a control of gene expression depends particularly on the specific binding of an oligomer sequence to a gene. Hence, to develop oligonucleotide-forming triplexes as therapeutic agents, it is necessary to have a clear understanding of how the

* To whom correspondence should be addressed. Phone: (402) 559-4628. Fax: (402) 559-9543. E-mail: lmarky@unmc.edu.

[†] Departments of Pharmaceutical Sciences and Biochemistry and Molecular Biology.

[‡] Eppley Institute for Cancer Research.

10.1021/jp052327y CCC: $30.25
Published on Web 09/07/2005

CHART 1: Oligomer Sequences and Their Designations

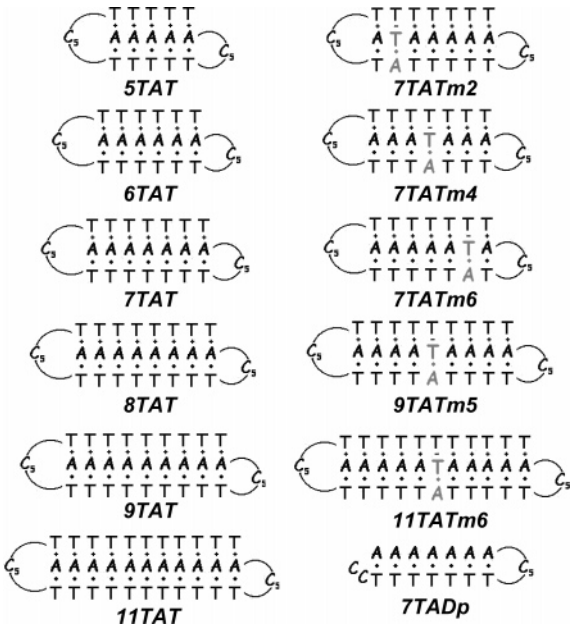

sequence, base composition, and solution conditions affect triplex stability. To further our understanding on the physical chemical properties of DNA triplexes, we have studied a set of intramolecular triplexes with exclusively TAT base triplets. The use of intramolecular structures simplifies the study of triple helices because they are more stable than their bimolecular and trimolecular counterparts due to a lower entropy penalty in their formation.[14] Furthermore, these intramolecular triplexes resemble that of H-DNA without the dangling strand, which can potentially form due to the high frequency of homopurine/homopyrimidine sequences in the human genome.[15] Sequences capable of forming H-DNA are present in regions that function in transfection, replication, recombination, and regulation of some eukaryotic genes.[5,7] In principle, a synthetic DNA strand designed to pair with these sequences forming a local triplex could disrupt gene expression. Therefore, the study of intramolecular triplexes might further the knowledge of the formation of H-DNA complexes.

In this report, we have used a combination of optical and calorimetric techniques to investigate the melting behavior of intramolecular DNA triplexes. We evaluate the thermodynamic consequences for the incorporation of 5−11 TAT base triplets and how strict the homopurine/homopyrimidine requirement of these triplexes is. This requirement is tested by the inclusion of single AT → TA substitution at different positions in the duplex stem and by the incorporation of additional flanking TAT base triplets around the substitution (Chart 1). Our results show that the formation of a base-triplet stack is driven by a large and favorable enthalpic contribution and that the effect for the incorporation of a single AT → TA substitution propagates through at least five base triplets to either side of the substitution, suggesting a high specificity upon triplex formation. Furthermore, electrostatic contributions, such as an increase in salt concentration, stabilize triplex formation.

Materials And Methods

Materials. All oligonucleotides were synthesized at the Eppley Institute Molecular Biology Core Facility at UNMC, reverse-phase HPLC purified, desalted on a G-10 Sephadex column, and lyophilized to dryness, prior to our experiments. The concentration of the oligomer solutions was determined at 260 nm and 80 °C using the following molar extinction coefficients in mM^{-1} cm^{-1} of strands: d($A_7C_5T_7C_2$), 197; d($A_5C_5T_5C_5T_5$), 220; d($A_6C_5T_6C_5T_6$), 246; d($A_7C_5T_7C_5T_7$), 273; d($A_8C_5T_8C_5T_8$), 307; d($A_9C_5T_9C_5T_9$), 336; d($A_{11}C_5T_{11}C_5T_{11}$), 394; d($ATA_5C_5T_5ATC_5T_7$), 282; d($A_5TAC_5TAT_5C_5T_7$), 282; d($A_3TA_3C_5T_3AT_3C_5T_7$), 282; d($A_4TA_4C_5T_4AT_4C_5T_9$), 340; and d($A_5TA_5C_5T_5AT_5C_5T_{11}$), 398. These values were calculated by extrapolation of the tabulated values of the dimers and monomer bases from 25 °C to high temperatures, using procedures reported earlier.[16] The buffer solutions consisted of 10 mM sodium phosphate buffer adjusted to different sodium concentrations with NaCl. All chemicals used in this study were reagent grade.

Circular Dichroism (CD) and UV Spectroscopies. To characterize the conformation of each DNA triplex, we prepared an oligonucleotide solution containing ~4 μM triplex in 10 mM phosphate buffer and 1.0 M NaCl. The CD spectrum was measured at 5 °C from 200 to 320 nm every 1 nm using a thermoelectrically controlled Aviv model 202SF circular dichroism spectrometer (Lakewood, NJ).

Absorbance versus temperature profiles (UV melting curves) as a function of strand and salt concentration were measured at 260 nm with a thermoelectrically controlled Aviv 14 DS ultraviolet−visible (UV−vis) spectrophotometer (Lakewood, NJ). The absorbance was scanned with a temperature ramp of ~0.4 °C/min. The analysis of the shape of the melting curves yielded transition temperatures, T_Ms, which correspond to the inflection point of the order−disorder transitions. To determine the molecularity of these triplexes, we investigated the T_M dependence as a function of strand concentration with the total strand concentration ranging from 1.6 to 150 μM.

Differential Scanning Calorimetry (DSC). Heat capacity functions of the helix−coil transition of each triplex were measured with a Microcal VP-DSC (Northampton, MA) instrument. Two cells, the sample cell containing 0.5 mL of a DNA solution (~0.15 mM in total strands) and the reference cell filled with the same volume of buffer solution, were heated from 0 to 90 °C at a heating rate of 0.75 °C/min. Analysis of the resulting thermographs yielded T_Ms and standard thermodynamic unfolding profiles: ΔH_{cal}, ΔS_{cal}, and $\Delta G^\circ_{(T)}$.[17] These parameters are measured from DSC experiments using the following equations: $\Delta H_{cal} = \int \Delta C_p^a \, dT$ and $\Delta S_{cal} = \int (\Delta C_p^a/T) \, dT$, where ΔC_p^a represents the anomalous heat capacity during the unfolding process.[17] The free energy, $\Delta G^\circ_{(T)}$, is obtained at any temperature with the Gibbs relationship $\Delta G^\circ_{(T)} = \Delta H_{cal} - T\Delta S_{cal}$, assuming $\Delta C_p = 0$ between the initial and final states. Alternatively, $\Delta G^\circ_{(T)}$ can be obtained using the following relationship: $\Delta G^\circ_{(T)} = \Delta H_{cal}(1 - T/T_M)$, which can be applied rigorously for intramolecular transitions. Furthermore, to study the effect of salt upon triplex formation, we performed DSC experiments on oligomer solutions containing 0.1 and 1 M sodium chloride concentrations.

Results and Discussion

In the following sections, we first describe in general the thermodynamic behavior of "TAT" triplexes followed by a discussion of the pyrimidine motif, thermodynamic contributions for the inclusion of TAT base triplets, AT → TA substitutions, and the increase of flanking TAT base triplets around the substitution.

Circular Dichroism. Analysis of the CD spectra (Figure 1) indicates that all triplexes and the control duplex exhibit the typical spectra of a nucleic acid helix in the "B" conformation;

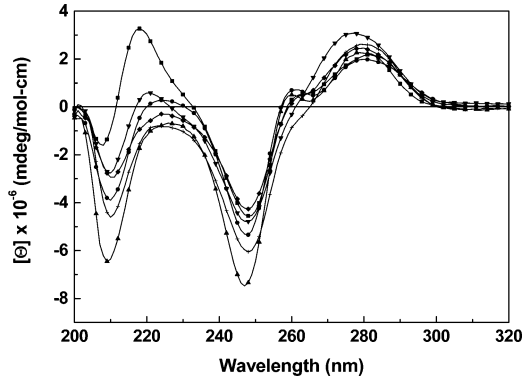

Figure 1. Typical CD spectra in 10 mM sodium phosphate buffer and 1.0 M NaCl at pH 7.0: *7TADp* (squares), *7TAT* (circles), *9TAT* (up triangles), *7TATm2* (down triangles), *7TATm6* (diamonds), and *9TATm5* (crosses).

that is, the positive band centered at ∼277 nm has a magnitude comparable to that of the negative band at ∼246 nm. This indicates that binding of the third strand does not impose major distortions in the duplex geometry. Furthermore, the small split of the positive band, 260−265 nm, is characteristic of the homopurine/homopyrimidine sequences (A_n/T_n) used in this work. All triplexes exhibit increased negative bands at 210 and 247 nm, when compared to the control duplex (*7TADp*). The 210 nm band has also been observed in previous reports,[18−20] and it has been considered as a characteristic feature of the formation of triple helices, while the band at 247 nm indicates additional base stacking interactions of the third strand.

UV Melting Curves. The helix−coil transition of each triplex and control duplex is characterized initially by UV melting techniques. Figure 2a shows typical melting curves for some of these triplexes. These curves follow the characteristic sigmoidal behavior for the unfolding of a nucleic acid helix, and their hyperchromicity increases with an increase in the number of base triplets. The UV melts of the duplex hairpin (*7TADp*) exhibit monophasic transitions under all conditions, consistent with previous reports.[21,22] However, the unfolding of some triplexes showed monophasic or biphasic behavior depending on the number of TAT base triplets in the stem and the incorporation of AT → TA substitutions.

To determine the molecularity of each triplex, we follow the transition temperature as a function of strand concentration. The T_M dependence on strand concentration is shown in Figure 2b for the unfolding of some triplexes. All molecules yielded similar T_Ms over a 100-fold increase in strand concentration, confirming their intramolecular formation. The use of intramolecular hairpins presents several advantages. For instance, they are thermally more stable than their bimolecular and trimolecular counterparts because their formation takes place at a lower entropy cost. In addition, these triplexes also formed at low sodium concentrations, allowing us to study their physical properties in a wide variety of solution conditions. Therefore, all molecules were designed to fold into intramolecular structures.

DSC Melting Curves. DSC experiments were conducted at two different NaCl concentrations, 0.1 and 1.0 M. The pH of 7.0 was maintained constant, because the formation of TAT base triplets is independent of pH.[19] DSC melts under these conditions indicate that these molecules melt in monophasic (triplex or duplex → random coil) or biphasic (triplex → duplex → random coil) transitions. The melting behavior depends on the number of TAT base triplets on the stem, incorporation of the AT → TA substitution, and the concentration of salt used.

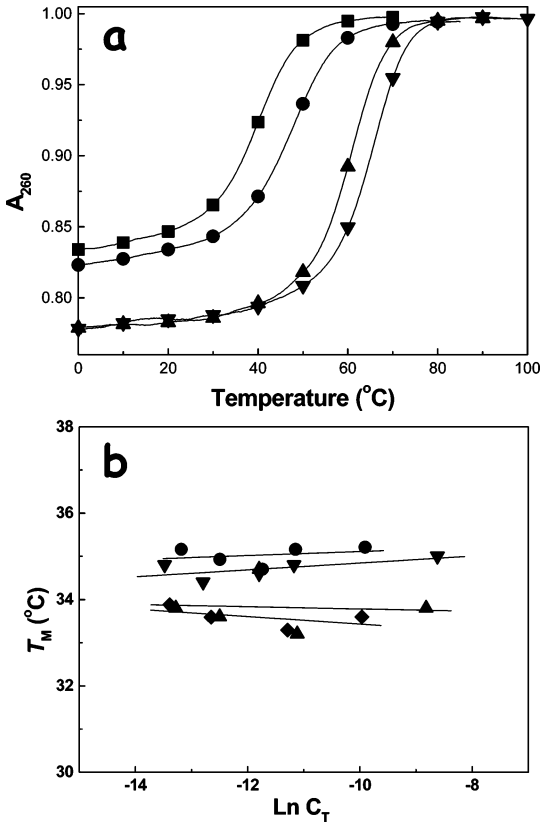

Figure 2. (a) Typical UV melting curves in 10 mM sodium phosphate buffer at pH 7 and 1.0 M NaCl: *5TAT* (squares), *7TAT* (circles), *9TAT* (up triangles), and *11TAT* (down triangles). (b) T_M dependences on strand concentration (2−200 μM): *7TAT* (circles), *7TATm6* (diamonds), *9TAT* (up triangles), and *11TAT* (down triangles).

In general, the incremental incorporation of TAT base triplets yielded triplexes with larger unfolding heats and higher T_Ms (Figure 3), while the incorporation of a AT → TA substitution decreased the enthalpic contribution as well as the thermal stability (see Figure 4). For all triplexes, the increase in the salt concentration yielded DSC melting curves with higher T_M's and slightly lower enthalpies. This indirectly suggests the presence of heat capacity effects in the unfolding of these triplexes.

Furthermore, the higher T_Ms with the increase in the concentration of sodium are consistent with the higher screening of the negatively charged phosphates. This is physiologically relevant because, in addition to sodium ions, the presence of other ions in the cell might help in triplex formation. Since the local concentration of condensed ions at the triplex surface is more or less constant,[23] the reason for this stabilizing effect is through a charge or Debye−Hückel screening effect. This effect yields perhaps a net improvement of stacking interactions which is compensated with a displacement of water molecules. However, an increase in the concentration of sodium from 0.1 to 1.0 M decreases their unfolding enthalpy by an average of ∼6.1 kcal/mol, possibly because the increase in sodium lowers the activity of water, enough to change the overall hydration state of these triplexes. Alternatively, immobilized electrostricted water molecules that contribute to the unfolding enthalpy are being replaced by sodium ions.

Thermodynamic Profiles. Tables 1−3 show complete unfolding thermodynamic profiles for all of the oligomers studied. Analysis of the data indicates that the folding (negative of the values in Tables 1−3) of each molecule at 20 °C is accompanied by a favorable free energy term resulting from the characteristic compensation of favorable enthalpy terms and

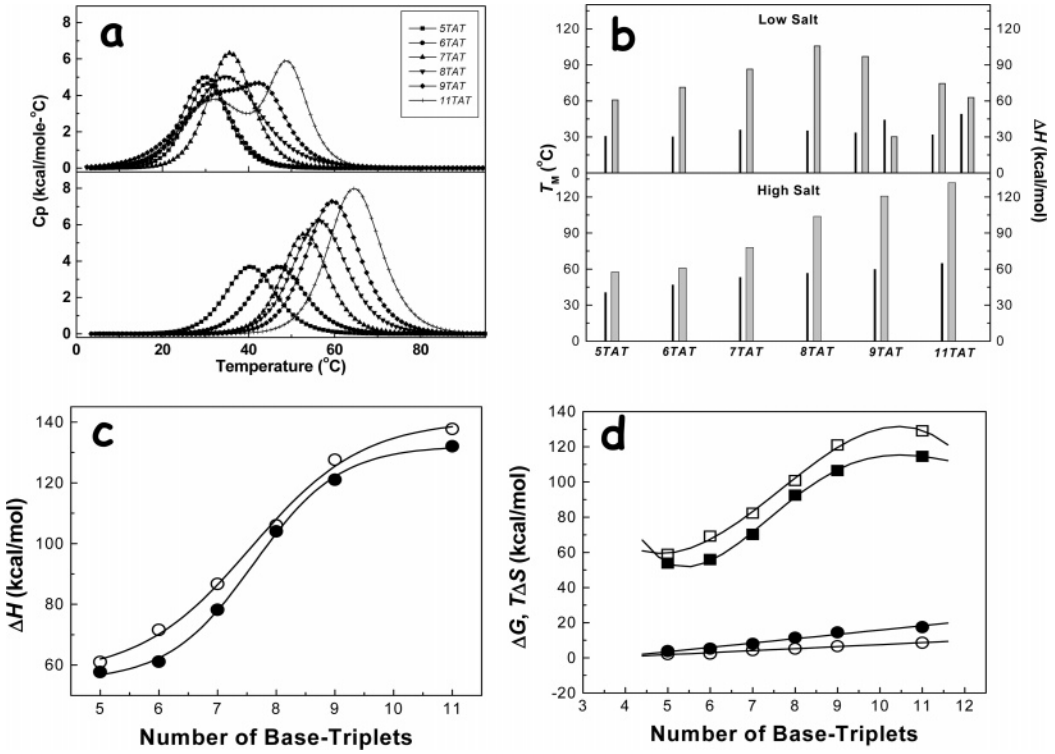

Figure 3. (a) DSC melting curves of triplexes in 10 mM sodium phosphate buffer at pH 7 and 0.1 M NaCl (upper curves) or 1.0 M NaCl (lower curves). (b) Thermodynamic contributions for the incorporation of TAT base triplets in intramolecular triplexes. T_M (black bars) and ΔH for each transition (gray bars). (c) The dependence of the total ΔH value on the number of base triplets: 0.1 M NaCl (open circles) and 1.0 M NaCl (solid circles). (d) The dependence of $\Delta G°$ (circles) or $T\Delta S$ (squares) on the number of base triplets: 0.1 M NaCl (open symbols) and 1.0 M NaCl (solid symbols).

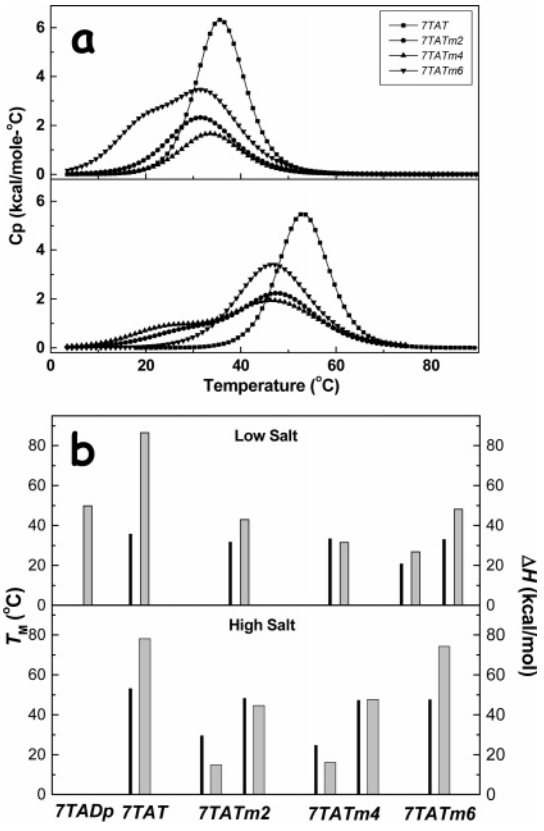

Figure 4. (a) DSC melting curves of single substituted triplexes as a function of the position of the AT → TA substitution in 10 mM sodium phosphate buffer at pH 7 and 0.1 M NaCl (upper curves) or 1.0 M NaCl (lower curves). (b) Unfolding thermodynamic parameters, T_M (black bars), and ΔH for each transition (gray bars).

unfavorable entropy terms. The favorable enthalpy terms correspond mainly to heat contributions from the formation of base-pair stacks, and/or base-triplet stacks, and hydrogen bonding,[19] while the unfavorable entropy terms arise from contributions of the unfavorable ordering of strands and the uptake of counterions and water molecules.[19]

Further analysis of the data (Tables 1−3) shows that the driving force for triplex formation is a large and favorable enthalpy change. Relative to its control *7TADp* duplex, the *7TAT* triplex has larger enthalpic contributions, by 39.3 kcal/mol (0.1 M NaCl) and 35.4 kcal/mol (1 M NaCl), which is due to the association of the third strand. This enthalpic contribution can be explained by the formation of Hoogsteen hydrogen bonds and base stacking interactions among the pyrimidines of the third strand, consistent with the formation of a triple helix. In this salt range, an average enthalpy of 6.2 kcal/mol is estimated for a single T/T base stack (37.3/6) of the thymine strand in the triple helical state, which is comparable to 5.2 kcal/mol obtained by Kamiya using isothermal titration calorimetry (ITC).[24] Although, different and independent methods were used, the values obtained by Kamiya and our values are close, which indicates a reliable estimate for a T/T base stack. The discrepancy between these two values may arise from base stacking contributions that are present at the lower temperatures used in the ITC experiments. Although Kamiya's triplex is a mixture of thymines and cytosines, we can assume equivalent stacking interactions due to their similar aromatic ring system.

Furthermore, comparison of model dependent van't Hoff enthalpies, ΔH_{vH}, compared to their corresponding calorimetric enthalpies, ΔH_{cal}, yields an average $\Delta H_{vH}/\Delta H_{cal}$ ratio of 0.63, indicating that the unfolding of these triplexes is not in a two-state fashion; that is, intermediate states are present during their

TABLE 1: Thermodynamic Unfolding Profiles for the Incremental Incorporation of TAT Base Triplets at 20 °C[a]

0.1 M NaCl					1.0 M NaCl				
T_M	$\Delta G_{(20)}$	ΔH_{cal}	ΔH_{vH}	$T\Delta S$	T_M	$\Delta G_{(20)}$	ΔH_{cal}	ΔH_{vH}	$T\Delta S$
				5TAT					
30.6	2.1	61.0	56.0	58.9	40.6	3.8	57.7	50.0	53.9
				6TAT					
30.2	2.4	71.6	50.0	69.2	47.0	5.2	61.1	49.0	55.9
				7TAT					
35.8	4.4	86.7	55.0	82.3	53.2	8.0	78.2	59.0	70.2
				8TAT					
35.2	5.2	106.0	35.5	100.8	56.6	11.5	104.0	51.6	92.5
				9TAT					
33.5	4.3	97.2	45.2	92.9					
44.3	2.3	30.4	55.4	28.1	59.8	14.5	121.0	53.5	106.5
				11TAT					
32.0	2.9	74.7	43.2	71.8					
49.2	5.7	63.0	62.7	57.3	64.7	17.5	132.0	56.0	114.5

[a] The presence of two rows for a given triplex molecule indicates biphasic transitions. The T_Ms are given in °C, while all other parameters, in kcal/mol (1 cal = 4.18 J). All parameters are measured in 10 mM sodium phosphate buffer at pH 7.0 with 0.1 or 1.0 M NaCl. Experimental uncertainties are as follows: T_M (±0.5 °C), $\Delta G°$ (±5%), ΔH_{cal} (±5%), ΔH_{vH} (±15%), and $T\Delta S$ (±7%).

TABLE 2: Thermodynamic Unfolding Profiles for the Incorporation of AT → TA Substitutions into Different Positions of the Duplex Stem at 20 °C[a]

0.1 M NaCl					1.0 M NaCl				
T_M	$\Delta G_{(20)}$	ΔH_{cal}	ΔH_{vH}	$T\Delta S$	T_M	$\Delta G_{(20)}$	ΔH_{cal}	ΔH_{vH}	$T\Delta S$
				7TADp					
35.2	2.3	47.4	39.2	45.1	52.6	4.3	42.8	40.0	38.5
				7TAT					
35.8	4.4	86.7	55.0	82.3	53.2	8.0	78.2	59.0	70.2
				7TATm2					
31.7	1.7	43.1	39.0	41.4	29.5	0.5	15.0	31.0	14.5
					48.3	3.9	44.7	40.0	40.8
				7TATm4					
33.4	1.2	28.2	45.0	27.0	24.8	0.3	16.1	33.0	15.8
					47.3	4.1	47.8	32.0	43.7
				7TATm6					
20.9	0.1	26.9	42.0	26.8	47.6	6.4	74.4	39.0	68.0
33.1	2.1	48.3	40.0	46.2					

[a] The presence of two rows for a given triplex molecule indicates biphasic transitions. The T_Ms are given in °C, while all other parameters, in kcal/mol (1 cal = 4.18 J). All parameters are measured in 10 mM sodium phosphate buffer at pH 7.0 with 0.1 or 1.0 M NaCl. Experimental uncertainties are as follows: T_M (±0.5 °C), $\Delta G°$ (±5%), ΔH_{cal} (±5%), ΔH_{vH} (±15%), and $T\Delta S$ (±7%).

unfolding which is comparable with the ratio obtained by Soto et al.[25]

Contribution of TAT Base Triplets and TAT/TAT Base-Triplet Stacks. To investigate the energetic contribution for the incorporation of TAT base triplets upon triplex formation, we investigated a set of DNA intramolecular triplexes containing 5−11 TAT base triplets in their stem, triplexes in the first column of Chart 1. As we increase the number of TAT base triplets, their T_Ms and total ΔH increase, which is consistent with the formation of additional base-triplet stacks (Table 1). Specifically, in 0.1 M NaCl (upper plots of Figure 3a and b), the melting behavior of *5TAT*, *6TAT*, *7TAT*, and *8TAT* is monophasic, while *9TAT* and *11TAT* showed biphasic transitions. However, upon an increase of salt concentration to 1.0 M NaCl (bottom plots of Figure 3a and b), the *9TAT* and *11TAT* triplexes change their melting behavior from biphasic to monophasic, indicating that salt induces the formation of stronger triplexes. The T_M and total enthalpy values increased with an increase in the number of base triplets; similar findings have been reported elsewhere.[20] However, this stepwise increment is not linear. Moreover, a plot of the total ΔH changes of all transitions as a function of the number of base triplets in the stem follows a sigmoidal curve, as shown in Figure 3c. The increment in enthalpy from triplex *5TAT* to *6TAT* is small (~10.6 kcal/mol), becomes larger *7TAT* through *9TAT* (~20 kcal/mol), and levels off between *9TAT* and *11TAT* (~10 kcal/mol). We explain these observations in terms of the formation of these triplexes (opposite sign of the thermodynamic parameters shown in Figure 3b−d) as follows: triplexes with less than four TAT base triplets in the stem most likely do not form because this short stem is not long enough to overcome the entropy driven nucleation step. The intercept of the two lines with the free energy axis of Figure 3d takes place at four TAT base triplets. The DSC melting curve (data not shown) of the potential triplex with four TAT base triplets indicates that this triplex does not form; the magnitude of the enthalpy (21 kcal/mol) corresponds to the unfolding of a monomolecular duplex with four AT base pairs, thus confirming our observation of Figure 3d. However, *5TAT* overcomes this nucleation step with a compensating enthalpy contribution; thus, the observed enthalpy is less favorable. As the formation of TAT base triplets increases, the enthalpy contribution for a single step becomes larger than its counterpart entropic contribution (see Figure 3c and d). The additional incorporation of base triplets to 9, and then 11, may cause the formation of triplexes with a lower number of TAT/TAT base-triplet stacks, presumably by slipping the third strand toward the formation of larger loops; that is, the loops will also include thymine residues.

TABLE 3: Thermodynamic Unfolding Profiles for the Incorporation of Flanking TAT Triplets around a AT → TA Substitution at 20 °C[a]

0.1 M NaCl					1.0 M NaCl				
T_M	$\Delta G_{(20)}$	ΔH_{cal}	ΔH_{vH}	$T\Delta S$	T_M	$\Delta G_{(20)}$	ΔH_{cal}	ΔH_{vH}	$T\Delta S$
				7TATm4					
33.4	1.2	28.2	45.0	27.0	24.8	0.3	16.1	33.0	15.8
					47.3	4.1	47.8	32.0	43.7
				9TATm5					
42.7	4.0	55.0	50.0	51.0	34.3	1.7	37.2	32.0	35.5
					57.0	6.9	61.3	52.0	54.4
				11TATm6					
46.7	6.4	76.6	56.0	70.2	40.9	4.1	61.6	26.0	57.5
					63.0	7.6	59.6	69.0	52.0

[a] The presence of two rows for a given triplex molecule indicates biphasic transitions. The T_Ms are given in °C, while all other parameters, in kcal/mol (1 cal = 4.18 J). All parameters are measured in 10 mM sodium phosphate buffer at pH 7.0 with 0.1 or 1.0 M NaCl. Experimental uncertainties are as follows: T_M (±0.5 °C), $\Delta G°$ (±5%), ΔH_{cal} (±5%), ΔH_{vH} (±15%), and $T\Delta S$ (±7%).

To calculate the enthalpic contribution of a single base-triplet stack, we use the plot of Figure 3c and the stepwise incremental of the linear portion of this figure (by averaging the heats of *7TAT*, *8TAT*, and *9TAT*); we obtained an enthalpic contribution of ~20.5 kcal/mol for the incorporation of an additional base-triplet stack, which is in excellent agreement with Soto's value of 24.4 kcal/mol.[25]

Furthermore, increasing the concentration of NaCl from 0.1 to 1 M NaCl yielded lower values of the unfolding enthalpies with higher T_Ms (Table 1). We observe a $\Delta\Delta H_{cal}$ value of −8.5 kcal/mol in this range of salt concentration for *7TAT*, and a similar molecule reported by Soto et al. yielded a $\Delta\Delta H_{cal}$ of

−7.6 kcal/mol.[19] This shows indirectly an average heat capacity effect of −505 cal/mol·°C with all of these triplexes. Kamiya et al. observed a heat capacity effect of −914 cal/mol; however, their reports are based on the analysis of an intermolecular 15-mer triplex and ITC analysis which may account for this difference.[24] A negative heat capacity effect in the unfolding of a macromolecule usually indicates a burial of hydrophobic surfaces. However, the unfolded state of a nucleic acid triplex is a random coil where the polar/nonpolar bases are more exposed to the solvent, yielding a more hydrophobic strand than their triplex state, so we invoke changes on the hydration state of the folded triplexes. In this range of salt concentration, the increase in salt concentration lowers the activity of water which in turns reduces the overall hydration of both triple helical and random coil states; however, salt has a larger effect on the helical state because of its higher charge density parameter; thus, the net effect is most likely a displacement of water molecules that are immobilized around charges (electrostricted water) from the triple helical state, and since energy is needed to remove this type of water,[26−29] a lower energy will be expected for the unfolding of these triplexes at 1 M NaCl. This displacement of water molecules by the additional association of sodium counterions is estimated from an average enthalpic difference of 6.1 kcal/mol (at 0.1 and 1 M NaCl) of all six triplexes and the energy (300 cal/mol of water) needed to remove electrostricted water;[19] we obtain a total average displacement of 20 water molecules/mol triplex. An alternative explanation is that the increase in salt stabilizes the W−C duplex of these molecules, destabilizing the association of the third strand; the net effect is an overall reduction of base−base stacking contributions in the third strand, which is consistent with a general rule on triplex formation that a strong duplex yields a weak triplex while a weak duplex yields a strong triplex.[30]

Figure 3d shows that the incorporation of additional TAT base triplets yields a linear increase in the $\Delta G^\circ_{(20)}$ values and the *Y*-intercept at $\Delta G^\circ_{(20)} = 0$ occurs at about four TAT base triplets; this means that the nucleation step for these triplexes is a minimum of four base triplets or three TAT/TAT base-triplet stacks. From the slopes of the two free energy lines (0.1 and 1 M NaCl) of Figure 3d, we obtain a $\Delta G^\circ_{(20)}$ value of 2.5 kcal/mol for the TAT/TAT base-triplet stack; then, we estimate a nucleation free energy, $\Delta G^\circ_{\text{nucleation}}$, at 20 °C of 7.5 kcal/mol compared to the nucleation free energy (2−3 kcal/ mol) for the formation of DNA duplexes.[31]

Single AT → TA Substitutions Placed in the W−C Duplex of *7TAT*. We have used the set of intramolecular triplexes with seven TAT base triplets to study the thermodynamic contribution for the substitution of a single AT → TA W−C base pair in different positions of the parent *7TAT* triplex; compare *7TAT* with *7TATm2*, *7TATm4*, and *7TATm6* of Chart 1. This incorporation yields DSC melting curves with monophasic or biphasic transitions (Figure 4) depending on the solution conditions and the position of the substitution. The resulting thermodynamic parameters are shown in Table 2. In 0.1 M NaCl, *7TATm2* and *7TATm4* exhibit monophasic transitions with 50−70% lower unfolding heats relative to *7TAT* but close to the heats of *7TADp* (control duplex) (Figure 4a), indicating these oligonucleotides are not forming triplexes and instead they formed duplexes with a floppy third strand. On the other hand, *7TATm6* unfolds in a biphasic fashion with a slightly lower unfolding heat than *7TAT*, which indicates a sequential melting behavior, triplex → duplex → coil. However, in 1.0 M NaCl, *7TATm2* and *7TATm4* exhibited biphasic transitions, while *7TATm6* unfolded in a monophasic fashion with similar total unfolding heats (both transitions) relative to *7TAT*. The $\Delta G^\circ_{(20)}$ terms are 1.6 kcal/mol (*7TATm6*) and 3.6 kcal/mol (*7TATm2* and *7TATm4*) less favorable than the $\Delta G^\circ_{(20)}$ value of *7TAT*; therefore, weaker triplexes are formed. To explain the biphasic melting behavior of *7TATm2* and *7TATm4*, we invoke their lower enthalpy contribution (relative to *7TAT*), but it is the coupling between the enthalpy and entropy terms that determines their cooperative melting behavior. The unsubstituted triplex has the right length of seven TAT base triplets, in which the third strand is well aligned in the major groove of the duplex, generating a hydrophobic spine in this groove, which is composed of a double chain of thymine methyl groups. The inclusion of the substituted TTA base triplet disrupts its compactness, due perhaps to the inability of the third strand thymine to reach its cognate adenine on the other side of the groove. Most likely, this thymine is stacked between adjacent thymines in this strand without forming Hoogsteen hydrogen bonds with the flipped adenine. In other words, the substitution modifies the overall association of the third strand with the duplex, yielding perhaps a more flexible triplex. A critical observation is that the increase in salt concentration from 0.1 to 1 M favors triplex formation; electrostatic contributions improve the screening of the negatively charged phosphates. An electrostatic free energy of 3.9 kcal/mol is estimated from the data of the two triplexes that formed at both salt concentrations (*7TAT* and *7TATm6*). Triplex formation is observed with *7TATm6* at both salt concentrations; one possibility is a triplex with five TAT base triplets, two W−C AT base pairs, and two end thymines that are frayed at the 3′ end; a second possibility is a similar triplex with the entire Hoogsteen strand slipped by two bases and forming a C_5T_2 loop at the 5′ end. Most likely, a combination of these two structures exists in solution.

In summary, the incorporation of an AT → TA substitution destabilizes triplex formation. This destabilization occurs because of the disruption of adjacent base-triplet stacks and may be explained as follows: The binding of the third strand thymine occurs asymmetrically within the major groove; that is, the thymine is displaced toward one side of the central axis, and in order for this thymine to bind to its cognate AT base pair, it has to follow the adenine to the other side of the major groove, that is, a movement of ∼11 Å, which may well create a disruption of adjacent base-triplet stacks, therefore compromising the overall formation of a triple helix.

Single AT → TA Substituted Triplexes with an Increasing Number of Flanking TAT Base Triplets. In the previous sections, we have estimated a nucleation step of four TAT base triplets for the formation of these pyrimidine triplexes. Therefore, to study the effect of flanking base triplets around a single AT → TA substitution, we have incorporated up to 10 TAT base triplets in triplexes containing a single AT → TA substitution, five to either side of the substitution. Specifically, we investigated the following triplex molecules: *7TATm4*, *9TATm5*, and *11TATm6* containing three, four, and five flanking TAT base triplets around the substitution, respectively (Chart 1).

The incorporation of flanking TAT base triplets increases the stability of the molecules (see Table 3). At low salt concentration, their DSC melting curves yielded monophasic transitions with unfolding heats significantly low (40−70%) relative to their parent triplexes (*7TAT*, *9TAT*, and *11TAT*), which indicates the sole formation of a duplex structure (Figure 5). Therefore, we suggest that the destabilizing effect for the incorporation of a single AT → TA substitution at the center of each triplex propagates up to at least five flanking TAT base triplets,

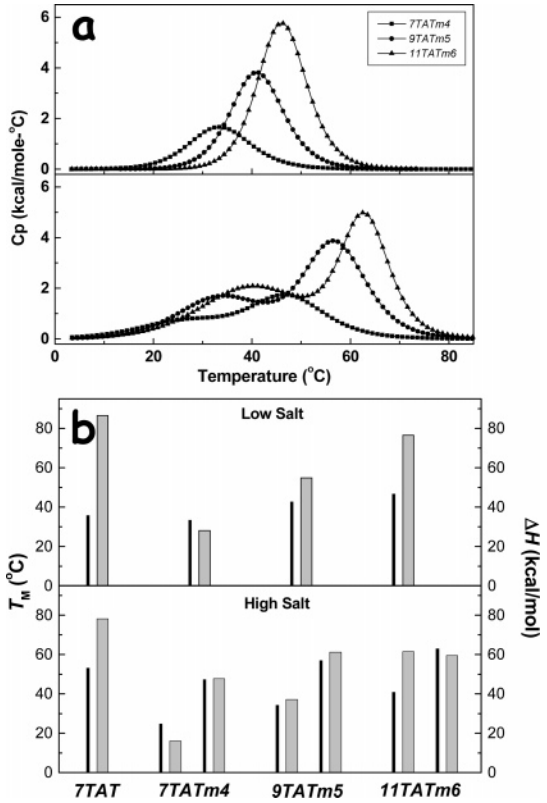

Figure 5. (a) DSC melting curves of single substituted triplexes as a function of the number of TAT flanking base triplets in 10 mM sodium phosphate buffer at pH 7 and 0.1 M NaCl (upper curves) or 1.0 M NaCl (lower curves). (b) Unfolding thermodynamic parameters, T_M (black bars), and ΔH for each transition (gray bars).

indicating a high specificity upon triplex formation. However, upon an increase in salt concentration to 1.0 M NaCl, biphasic transitions are observed that correspond to the unfolding of weak triplexes. Similarly to previous sections, additional electrostatic contributions stabilized triplex formation. Analysis of the thermodynamic profiles in 1 M NaCl shows an ~40% decrease in $\Delta G^\circ_{(20)}$ relative to their respective parent triplexes (*7TAT*, *9TAT*, and *11TAT*) (Tables 1 and 3). This shows that counterions stabilize the formation of triplexes. However, there might not be a true TAT base-triplet formation with the AT → TA substituted base pair, since weaker triplexes are formed. The additional enthalpy contribution (obtained at 1 M relative to 0.1 M NaCl) could be explained by the thymine contributing base stacking interactions with adjacent thymines.

Conclusions

We have investigated the melting behavior of double hairpin triplexes of the pyrimidine motif containing exclusively TAT base triplets as a function of salt concentration. Specifically, we have studied their melting behavior as a function of the number of TAT base triplets and the thermodynamic effects for the disruption of the homopurine/homopyrimidine requirement of these triplexes, by incorporating both single AT → TA substitutions in the duplex domain and additional TAT base triplets flanking this type of substitution.

The melting behavior of these triplexes were monophasic or biphasic depending on the number of TAT base triplets and the presence and location of the AT → TA substitution, and unfolding took place through the formation of intermediate states. The results indicate that their melting behavior is consistent with an enthalpy−entropy balance between duplex and triplex formation. A minimum of five TAT base triplets is needed to form stable intramolecular triplexes in the B-like conformation; however, the increase of base triplets to 9 or 11 causes strand slipping, generating triplexes with a lower number of TAT base triplets in the stem and larger cytosine loops.

The incorporation of a single AT → TA substitution decreases triplex stability due to the disruption of favorable base-triplet stacking interactions around the substitution; this destabilizing effect compromises the overall compactness of the molecule. However, the increase of the ionic strength yields a net improvement of their stacking contributions due to the higher screening of the negatively charged phosphates. The results showed that stable pyrimidine triplexes form when their duplex segments are composed of homopurine/homopyrimidine sequences. This suggests a high specificity upon binding of the third strand to a DNA duplex. Furthermore, these intramolecular triplexes resemble that of an H-DNA molecule without the dangling fourth strand which is present in human DNA, and the overall thermodynamic results are consistent with their in vivo formation.

Acknowledgment. This work was supported by grant MCB-0315746 from the National Science Foundation. We thank Prof. Vinod Labhasetwar for editorial assistance.

References and Notes

(1) Juliano, R. L.; Astriab-Fisher, A.; Falke, D. *Mol. Interventions* **2001**, *1*, 40.
(2) Crooke, S. T. *Biochim. Biophys. Acta* **1999**, *1489*, 31.
(3) Helene, C. *Eur. J. Cancer* **1991**, *27*, 1466.
(4) Helene, C. *Eur. J. Cancer* **1994**, *30A*, 1721.
(5) Praseuth, D.; Guieysse, A. L.; Helene, C. *Biochim. Biophys. Acta* **1999**, *1489*, 181.
(6) Thuong, N. T.; Helene, C. *Angew. Chem., Int. Ed. Engl.* **1993**, *32*, 666.
(7) Soyfer, V. N.; Potaman, V. N. *Triple-Helical Nucleic Acids*; Springer-Verlag: New York, 1996.
(8) Maher, L. J. I.; Wold, B.; Dervan, P. B. *Science* **1989**, *245*, 725.
(9) Neidle, S. *Anti-Cancer Drug Des.* **1997**, *12*, 433.
(10) Brown, P. M.; Madden, C. A.; Fox, K. R. *Biochemistry* **1998**, *37*, 16139.
(11) Cheng, Y. K.; Pettitt, B. M. *Prog. Biophys. Mol. Biol.* **1992**, *58*, 225.
(12) Keppler, M. D.; Fox, K. R. *Nucleic Acids Res.* **1997**, *25*, 4644.
(13) Beal, P. A.; Dervan, P. B. *Science* **1991**, *251*, 1360.
(14) Chen, F. M. *Biochemistry* **1991**, *30*, 4472.
(15) Schroth, G. P.; Ho, P. S. *Nucleic Acids Res.* **1995**, *23*, 1977.
(16) Marky, L. A.; Blumenfeld, K. S. *Biopolymers* **1983**, *22*, 1247.
(17) Marky, L. A.; Breslauer, K. J. *Biopolymers* **1987**, *26*, 1601.
(18) Plum, G. E.; Breslauer, K. J. *J. Mol. Biol.* **1995**, *248*, 679.
(19) Soto, A. M. Thermodynamic for the Unfolding of Non-Canonical Nucleic Acids: Bent Duplexes, Okazaki Fragments, and DNA Triplexes. Doctoral Dissertation, University of Nebraska Medical Center, Omaha, NE, 2002.
(20) Soto, A. M.; Marky, L. A. *Biochemistry* **2002**, *41*, 12475.
(21) Rentzeperis, D. Thermodynamics and Ligand Interactions of DNA Hairpins. Doctoral Dissertation, New York University, New York, 1994; p 246.
(22) Rentzeperis, D.; Marky, L. A. *J. Am. Chem. Soc.* **1995**, *117*, 5423.
(23) Manning, G. *Q. Rev. Biophys.* **1978**, *11*, 179.
(24) Kamiya, M.; Torigoe, H.; Shindo, H.; Sarai, A. *J. Am. Chem. Soc.* **1996**, *118*, 4532.
(25) Soto, A. M.; Loo, J.; Marky, L. A. *J. Am. Chem. Soc.* **2002**, *124*, 14355.
(26) Rentzeperis, D.; Shikiya, R.; Maiti, S.; Ho, J.; Marky, L. A. *J. Phys. Chem. B* **2002**, *106*, 9945.
(27) Conway, B. E. *Ionic Hydration in Chemistry and Biophysics*; Elsevier: New York, 1981.
(28) Tunis, M. J.; Hearst, J. E. *Biopolymers* **1968**, *6*, 1325.
(29) Tunis, M. J.; Hearst, J. E. *Biopolymers* **1968**, *6*, 1345.
(30) Roberts, R. W.; Crothers, D. M. *Science* **1992**, *258*, 1463.
(31) SantaLucia, J. J.; Allawi, H. T.; Seneviratne, A. *Biochemistry* **1996**, *35*, 3555.